# Patients Lung Derived Tumoroids (PLDTs) to model therapeutic response

Frederic Delom, Inaki Begiristain, Thomas Grenier, Hugues Begueret, Fabienne Soulet, Géraldine Siegfried, Abdel-Majid Khatib, Jacques Robert, Delphine Fessart

# Patients Lung Derived Tumoroids (PLDTs) to model therapeutic response

Frederic Delom[3*], Inaki Begiristain[3ǂ], Thomas Grenier[3ǂ], Hugues Begueret[3,4], Fabienne Soulet[5,6], Geraldine Siegfried[5,6], Abdel-Majid Khatib [5,6], Jacques Robert [3] and Delphine Fessart [1,2,3]*

[1]INSERM U1242, "Chemistry, Oncogenesis Stress Signaling", Univ. Rennes 1, F-35000 Rennes, France; [2]Centre de Lutte Contre le Cancer Eugène Marquis, F-35000 Rennes, France; [3] ARTiSt Group, Univ. Bordeaux, INSERM, Institut Bergonié, ACTION, U1218, F-33000 Bordeaux, France; [4]Hôpital Haut-Lévêque, CHU de Bordeaux, avenue de Magellan, 33604 Pessac cedex, France. [5]Université de Bordeaux, Bordeaux, France ; [6]INSERM UMR1029, 33400 Pessac, France.

ǂ Equally contributed

***Correspondence to:**

DF - E-mail: delphine.fessart@inserm.fr or FD - E-mail: frederic.delom@yahoo.fr

**Key words**: Tumoroids, Three-dimensional culture, Radiation, Chemotherapeutic drugs, Lung cancer.

**Abstract**

Preclinical lung cancer models are essential for a basic understanding of lung cancer biology and its translation into efficient treatment options for affected patients. Lung cancer cell lines and xenografts derived directly from human lung tumors have proven highly valuable in fundamental oncology research and anticancer drug discovery. Both models inherently comprise advantages and caveats that have to be accounted for. Recently, we have enabled reliable *in vitro* culture techniques from lung cancer biopsies as Patients Lung Derived Tumoroids (PLDTs). This breakthrough provides the possibility of high-throughput drug screening covering the spectrum of lung cancer phenotypes seen clinically. We have adapted and optimized our *in vitro* three-dimensional model as a preclinical lung cancer model to recapitulate the tumor microenvironment (TME) using matrix reconstitution. Hence, we developed directly PLDTs to screen for chemotherapeutics and radiation treatment. This original model will enable precision medicine to become a reality, allowing a given patient sample to be screened for effective *ex vivo* therapeutics, aiming at tailoring of treatments specific to that individual. Hence, this tool can enhance clinical outcomes and avoid morbidity due to ineffective therapies.

## 1. Introduction

Lung cancer is the most common cause of cancer-related mortality worldwide. Of lung cancer diagnosed, more than 80% are non small cell lung cancer (NSCLC), which includes adenocarcinoma, squamous cell carcinoma and large cell carcinoma [1]. The most common histological subtype of lung cancer is adenocarcinoma, accounting for almost half of all cancers [2, 3]. The majority of NSCLC patients are diagnosed during the later stages of lung cancer and dies without successful treatment [1, 4, 5].

One of the most difficulties in lung oncology is to develop a reliable model to assess the potential effects of candidate drugs. Preclinical research on anticancer drugs has the lowest success rate of all therapeutic areas, with 5% of candidate compounds having completed Phase III clinical safety and efficacy trials [6]. The most simplistic lung cancer models are bronchial cells derived from human and animal lung tumors grown as a flat monolayer in cell culture media. There is no doubt that immortalized lung tumor lines grown in 2D have contributed to a great deal of knowledge about the mechanisms leading to cancer development. However, in this monolayer model, lung cells adhere to an artificial substrate and are in contact with other cells only at the periphery. Thus lung cells cultured in flat layers on plastic surfaces do not reflect the multicellular microenvironment found in the bronchial tree. Animal models have been used as live incubators in which human lung tumors have been cultured, thus interacting with an entire organism, though often in an immune-depressed environment. Lung cancers have been established in rodent models by surgically implanting pulmonary tumor cells or by creating genetically modified animals that spontaneously develop human lung tumors in response to experimental modification of the expression of a specific gene. At first glance, this seems an inherently desirable system aiming at mimicking human lung cancer. Despite their intensive use for drug screening, these expensive animal models have not resulted in therapies translating into better outcomes of human cancer [7, 8]. Overall, these models have not generated therapies with a high return on investment.

For their fascinating potential as tools to probe human biology and disease, the journal Nature Methods has chosen organoids as “method of the year” in 2018 [9]. One of the most powerful aspects of organoids as research tools is how they have moved forward our understanding of human cancer biology. We have previously developed a 3D organoids/tumoroids tissue culture model from normal and malignant human lung epithelial cells [10]. Indeed, we have enabled a reliable *in vitro* model from lung cancer biopsies as Patient-Lung Derived Tumoroids (PLDTs) [10] to establish novel personalized lung cancer therapies. These therapies could define specific treatments for each patient on an individual basis. Using this method, we have characterized

organoids/tumoroids and showed that epithelial organization and many physiological cell-cell and cell-ECM contacts, cellular polarity, and secretory functions are preserved in epithelial organoids [10, 11]. Therefore, the tumoroids, in which cellular heterogeneity of tumor cells is preserved, have emerged as a promising tool. Recently, numerous studies highlighted the application of patient-derived tumoroids in personalized cancer medicine in terms of gene - drug association treatments, the identification of new therapies and the prediction of patient response. Thus using PLDT with similar characteristics to the original lung tumors may result in more accurate predictions of drug responses in patients. PLDTs have several advantages over pre-existing models, including conserving the molecular and cellular composition of the original tumor [12]. These advantages highlight the tremendous potential of PLDTs in personalized lung cancer therapy, particularly preclinical drug screening and predicting patient responses to selected treatment regimens.

In the present study, we have adapted and optimized our *in vitro* 3D model [10] as a potential personalized lung cancer medicine model. Personalized cancer medicine is an approach to tailoring effective therapeutics strategies for each patient according to a tumor genomic characterization. We have investigated the utility of our PLDT model in testing the activity of chemotherapeutic drugs alone or in combination with irradiation by comparing 2D *vs* 3D cultures of the same lung cancer cells obtained from biopsies of lung cancer patients. Herein, we show that PLDTs are more resistant to chemotherapeutic drugs and irradiation that cells in 2D culture. Thus, the PLDT model could enable precision medicine to become a reality, allowing patients samples to be screened for effective therapy, with the tailoring of treatments specific to each individual. Hence, this tool can enhance clinical outcomes by developing and delivering the right therapeutics, for the right cancer in the right patients. This would mean that outcome, morbidity, and ultimately survival should be improved for all patients with advanced lung cancer.

## 2. Materials and methods

*2.1 Cell isolation and cell lines culture*

Cancer lung epithelial cells obtained from tumor biopsies of patients were cultured in two different culture media: medium A containing 5 ng/ml epidermal growth factor (EGF), 50 µg/ml bovine pituitary extract (BPE) and 1% antibiotics mixt (100 IU/ml penicillin and 100 µg/ml streptomycin); and medium B supplemented with 15 µg/ml BPE, 10 ng/ml EGF, 0.5 µg/ml epinephrine, 5 µg/ml insulin, 10 µg/ml transferrin, 10 ng/ml triiodo-L-thyronine, 0.5 µg/ml hydrocortisone, 1.5 µg/ml albumin, 0.1 ng/ml retinoic acid, 1% Fetal Calf Serum (FCS) and 1% antibiotics mixt (100 IU/ml penicillin and 100 µg/ml streptomycin).

Samples of human lung cancer tissues were obtained from the Haut-Levêque University Hospital (Bordeaux, France) and reviewed by an expert pathologist in the field (H. Begueret) as previously published in [11]. These procedures were approved by the Institutional Review Board at Haut-Levêque University Hospital (NFS96900 Certification) in accordance with The Code of Ethics of the World Medical Association. Immediately after surgical resection, tumor biopsies were rinsed in Hank's Balanced Salt Solution (PAN Biotech) and cut in 2-3 mm pieces. For the explant culture, these pieces are placed in a 6-well plate, previously coated with a solution containing 30 µg/ml collagen, 10 µg/ml fibronectin and 10 µg/ml BSA. The explant was covered with a drop of culture medium (medium A or B) and incubated at 37°C, 5% $CO_2$. Then 2 ml of culture medium A or B was added to the explant. The culture medium was changed every 2 days. When the cells were confluent, they were detached from the plate with trypsin and seeded in 12-well plates.

For the enzymatic digestion, tissues from biopsies were rinsed in HBSS and cut into 2-3 mm pieces before being minced and incubated for 1 to 2 hours at 37°C in DMEM alone containing 50 to 1500 µl of collagenase I (Worthington). After digestion, the supernatant was recovered gently and filtered through a 40 µm filter. The samples were then centrifuged for 7 min at 4°C at 250 *g*. The pellet was taken up twice in DMEM alone and was centrifuged for 5 min at 4°C at 250 *g*. Finally, cells were taken up in culture medium A and seeded in a 6-well plate. Once the cells adhered to the support, the medium was changed every 2 days.

Two human cell lines were used: human fetal lung fibroblasts (IMR-90) and human embryonic kidney cells (HEK293). HEK293 were cultured in DMEM medium supplemented with 10% FBS and 1% antibiotics (100 IU/ml penicillin and 100 µg/ml streptomycin). The IMR-90 cells were cultured in Eagle MEM medium supplemented with 10% FBS, 1% L-glutamine and 1% antibiotics (100 IU/ml

penicillin and 100 µg/ml streptomycin). All cultures were kept in a humid incubator at 37°C and 5% $CO_2$. Sub-culturing was performed when the cells were 80% confluent.

*2.2 Chemotherapeutic assay in 2D monolayers*

Cells were seeded in triplicate at 5000 cells/mL in a 96-well plate and incubated at 37°C and 5% $CO_2$. Four days after seeding, cells were treated with concentrations of 0; 0.01; 0.1; 1; 10 and 100 µM of Docetaxel, Paclitaxel, Pemetrexed and Gemcitabine. To perform this treatment, 50% of the medium was replaced by complete DMEM medium supplemented with the chemotherapeutic agent. In parallel, untreated cellular control was performed. Three and five days after starting treatment, the cytotoxic effect of the four chemotherapeutic agents was measured by a cell viability assay (AlamarBlue). Briefly, AlamarBlue® solution was added to each well, 10% of the final volume, and the plate was incubated at 37°C, in the dark for 2 hours. After incubation, the absorbance was read at 570 and 600 nm using a spectrophotometer. The reduction percentage of AlamarBlue, corresponding to cell viability, was determined according to manufacturer instructions.

*2.3 Measuring response to Gemcitabine in soft-agar colony formation*

Colony formation efficiency was evaluated as previously described [11]. Briefly, cells were plated in medium supplemented with 3.3% FBS containing 0.35% soft agar in 6-wells plates over a layer of solidified medium containing 0.7% soft agar. Four days after seeding, cells were treated with concentrations of 0; 0.01; 0.1; 1; 10 and 100 µM of Gemcitabine. The medium was replaced with fresh Gemcitabine twice a week to maintain humidity. After growth, colonies were stained with Crystal Violet (0.05%) for 10 min and counted using a phase-contrast microscope (Leica) at objective 5×. The acquisition of images and their analysis were performed with the Leica software of the microscope (LAS X Software, Leica).

*2.4 Measuring response to Gemcitabine in 3D*

Cells were grown in 3D tumoroids according to our protocol [10, 11]. Briefly, the cells were seeded in a Matrigel matrix at the density of 2000 cells/$cm^2$ in a 96-well plate and incubated at 37°C and 5% $CO_2$. Treatment with chemotherapeutic agents began 4 days after seeding and was repeated at 7, 9 days. For each treatment, tumoroids were treated with concentrations of 0; 0.01; 0.1; 1; 10 and 100 µM Gemcitabine. For this purpose, 50% of the medium was replaced by a complete DMEM medium supplemented with the chemotherapeutic agent. In parallel, cellular control was performed with the vehicle. To calculate the number of tumoroids, a representative field in each condition was taken using a phase contrast-microscope (Leica) at objective 5×. The acquisition of a Z-stack (15 images) of each well and its analysis was performed with the Leica software of the microscope (LAS Software,

Leica). Briefly, for each multifocal image obtained with a Z-stack, we have applied a step-by-step analysis workflow containing 11 steps to obtain the organoid count and a size-wise classification. First, we selected the multifocal image, next we applied filters with gray processing followed by an enhancement of black objects set up to 14. The threshold was then adjusted to reduce the background noise. The image was then converted to binary processing for tumoroid detection. Once the new binary image was obtained, we have controlled that each tumoroid was recognized. We have then processed to the measurement of each tumoroid, and defined each tumoroid as an object, to automatically calculate the diameter and the number of each object. Afterward, we have classified the objects by size using 10 classes from the smaller tumoroid to the biggest one. Finally, we have obtained a histogram with the number of tumoroid per field and the diameter of tumoroids.

*2.5 Cell death assay*

Cells were seeded into a 96-well plate and grown for 4 days in 2D and 3D. After 4 days, cells were treated with different doses of Gemcitabine for 3 days. Cells were then stained for 30 min with NucBlue Live ReadyProbes Reagent (1 drop/ml media) and NucGreen Dead 488 ReadyProbes Reagent (1 drop/ml media) (ThermoFisher). The 96-well plate was imaged immediately. High-content images were acquired with the Cytation 3 automated microscope (Biotek) at 4× magnification, and analysis was performed using the Analysis software (Biotek). Cells were imaged simultaneously in the fluorescein isothiocyanate (FITC) (NucGreen) and 4', 6-diamidino-2-phenylindole (DAPI) (NucBlue) channels. A cell was defined as undergoing cell death when 50% or more of the nucleus, as defined by NucBlue-positive pixels, was overlapped by NucGreen-positive pixels.

*2.6 Chemoradiation in vitro studies*

Cells were seeded in 96 well format using a Perkin-Elmer Janus Mini liquid handling platform. Plates were incubated for the indicated times, and the medium was changed every two days. Tumoroids were plated in 96-well plates and allowed to grow for 1 day. Images were taken on a Leica DMi8 inverted microscope using a 4× objective before chemoradiation treatment. After imaging of monolayer or tumoroids, the medium was replaced with a feeding medium containing Gemcitabine at the desired concentrations, and tumoroids were subsequently exposed to ionizing radiation using an Xtrail XENX XSTRAHL Irradiator delivering a dose rate of approximately 0.75 Gy/minute. After 3 days, the culture medium was replaced with a standard medium. Before reading, cells in monolayers were incubated 30 minutes with Readyprobes blue (Invitrogen) for nuclei staining for live-cell imaging. High-content images were acquired with the Cytation 3 automated microscope (Biotek) at 4× magnification, and analysis was performed using the Analysis software (Biotek). All experiments were completed at least in triplicate.

*2.7 Immunofluorescence*

Cells were seeded on slides and incubated for 48 h at 37°C, 5% $CO_2$. After two PBS washes, cells were fixed for 15 min with 4% paraformaldehyde, followed by PBS wash before permeabilization with PBS 1×-0.1% NP40 for 15 min. Cells were then incubated with the appropriate primary antibody diluted in 1% BSA-0.5% Tween 20 for 1 h and then with the secondary antibody and with DAPI (4', 6'-diamidino-2-phenylindole). Finally, two washes were performed before mounting the slides in the mounting medium (Dako Fluorescent Mounting Medium). The different antibodies used were mouse anti-cytokeratin 18 (CK-18) monoclonal antibody (sc-32722, Santa Cruz), rabbit anti-Protein C (SP-C) rabbit polyclonal antibody (Ab 40879, Abcam) and mouse smooth muscle anti-actin (alpha-SMA) monoclonal antibody (A5228, Sigma). The secondary antibodies coupled were Alexa-fluor 488 goat anti-mouse (Life Technologies), the Alexa-fluor 546 anti-rabbit monkey (Life Technologies) and Alexa-fluor 546 goat anti-mouse (Life Technologies). After mounting the slides, slides were visualized with a Nikon Eclipse 2000-C1 confocal microscope and filters corresponding to the characteristics of the fluorochrome used, and the 20× and 60× immersion objectives. The images were then converted to Tiff format and analyzed using the Nikon EZ-C1 microscope software.

*2.8 Statistics*

Results are presented with a standard deviation of the mean in all studies. Statistical differences between each subtype of cancer were analyzed using a Student's t-test or ANOVA, as indicated, with GraphPad Prism 4 software. A p-value of 0.05 or less is considered significant. All experiments are compared to a control condition (cells only treated with the vehicle) to allow statistical comparisons.

## 3. Results

### *3.1 Patient-Lung Derived Tumoroid (PLDT) lines characteristics*

Recently, we have shown that PLDTs can be readily established from the majority of clinical tumor-containing NSCLC specimens tested [10]. Starting from January 2015 to February 2016, we collected a biopsy sample from 12 different lung cancer patients. The clinical characteristics of these patients are presented in Table 1. Known oncogenic mutations were sought in the genes *EGFR*, *KRAS*, *ERBB2*, *ALK*, *ROS1,* and *BRAF*, and mutations were detected for seven of the twelve patients (58.3%) (Table 1). Among these 7 samples, two had an *EGFR* mutation (CLC3 and CLC7) and five a *KRAS* mutation (CLC1, 6, 8, 9, 10). The histology included eleven adenocarcinoma and one squamous cell carcinoma (Table 1).

### *3.2 Human lung tumor cells isolation from biopsies by explant cell-culture.*

The primary explant technique is particularly useful for disaggregation of small quantities of tissues. The tissue in basal salt solution was finely chopped (Figure 1A, a), and washed by settlings. The basal salt solution was then removed. The tissue pieces were spread into 6-well plates and supplemented with two different types of mediums. The explants were attached to the bottom of the plate (Figure 1A, b) and observed periodically. After the addition of the appropriate medium, incubation was carried out for 3-8 days. When the outgrowth of tumor cells was observed (Figure 1A, c), cells were transferred into a fresh new dish for subculture (Figure 1B). This method requires serial sub-culturing to obtain primary lung tumor cell lines (Figure 1B). Explants of human bronchial tumor biopsies have been cultured in two different mediums: Medium A and Medium B (see Materials and methods) (Figure 1C-E). We have assessed the success rate of the establishment of patient-derived cell lines obtained with both mediums (Figure 1C). We then compared and evaluated the yield and the presence of epithelial cells for each medium. We observed a better yield with medium B (Figure 1D). The outgrowth of epithelial cells was observed within 6 to 8 days (Figure 1E). Taken together, these results show that human lung tumor cells grown from our explant cell culture method from patients' biopsies in medium B is suitable for developing primary lung tumor cell lines.

**Figure 1**

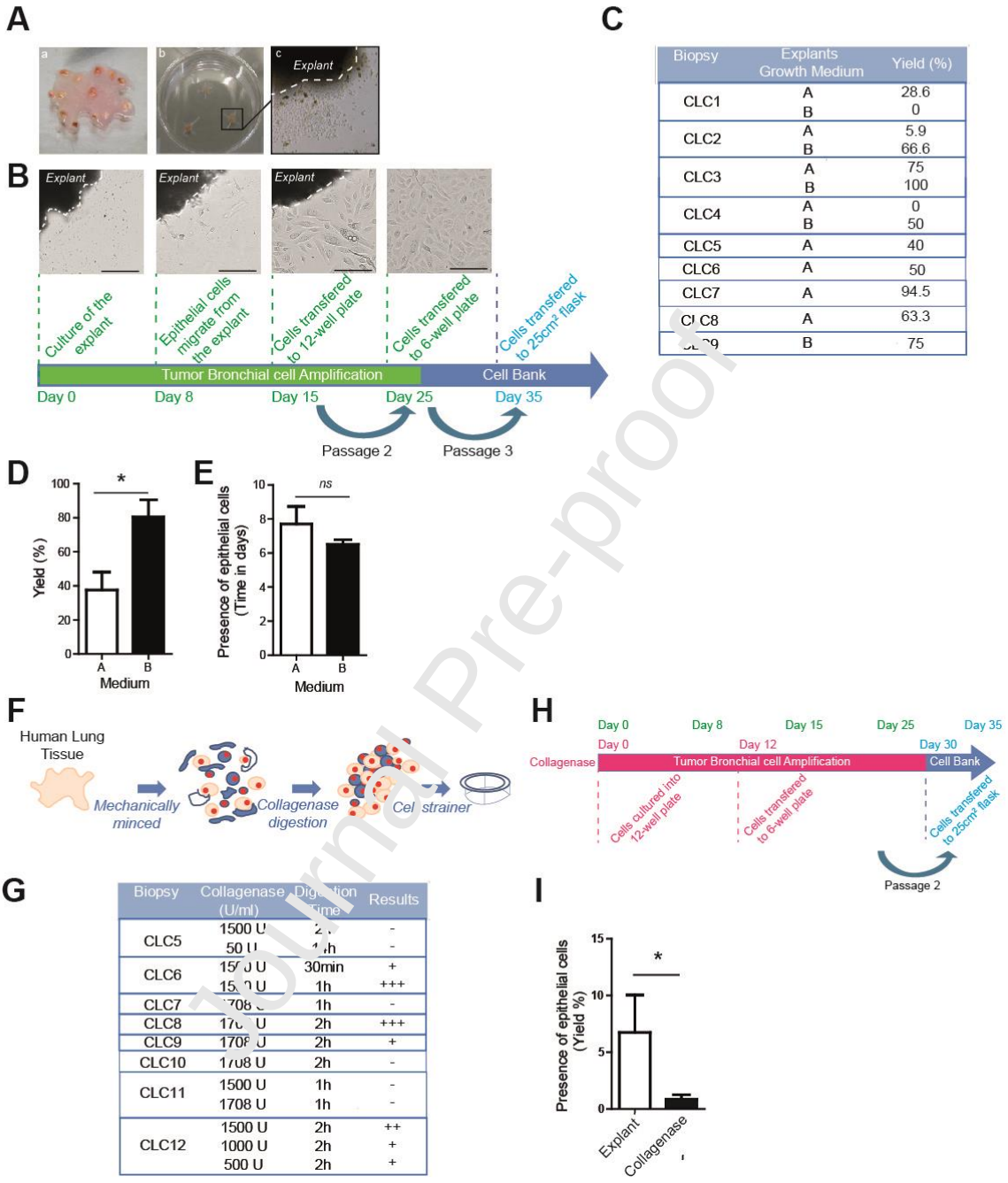


**Figure 1 Human bronchial tissue segments and freshly isolated lung cancer epithelial cells. A**, Representative picture of human bronchial tissue segments -~1-2 cm long and <1 cm diameter- (a) used for primary cultures of human lung epithelial cells. (b-c) Brightfield pictures representative of the outgrowth of the explant. **B**, Human lung epithelial cells grown from explants on tissue culture plates. Note the ring of cells of about 1-2 cm which becomes visible to the naked eye after 3-4 weeks. Images represent the edge of explant tissue and epithelial cells as they migrate from the explant, Scale bar=100 µm. The chronology illustrates the different steps to amplify cells. **C**, Table recapitulating the conditions assessed, two variables were tested: medium A and/or medium B for

each cancer lung cell line (CLC). **D**, The bar graph shows the yield in percentage of cells (mean ± s.e.m) obtained in Medium A as compared to Medium B from three independent biological replicates. *p<0.05 (Student's t-test). The yield in percentage of cells obtained with the explant was than calculated for each condition. **E**, Time in days to obtain primary lung cancer epithelial cells in their respective medium A *vs* B (mean ± s.e.m); from three independent biological replicates, n.s., non-significant. **F**, Schematic representation of the different steps to dissociate human lung tissue from biopsy with collagenase. **G**, Table recapitulating the conditions assessed, two variables were tested: the concentration of collagenase and the duration of collagenase treatment.( **–** ) no cells were growing, ( **+** ) some cells were growing, ( **++** ) few cells were growing to further expand, and ( **+++** ) a sufficient amount of cells were growing to further expand. **H**, The chronology illustrates the different steps required to expand cells either with the collagenase method (Pink). **I**, Yield in percentage of cells obtained with the explant as compared to collagenase (mean ± s.e.m from three independent biological replicates). *p<0.05 (Student's t-test).

*3.3 Human lung tumor cells isolation from biopsies by enzymatic digestion.*

Enzymatic dissociation is a commonly used practice to digest minced tissue into a single-cell suspension due to proper digestion of tissue and preservation of cell viability and integrity. Enzymatic disaggregation can be carried out by using trypsin, collagenase, or some other enzymes. Since numerous studies have shown that type I collagenase is more effective than other enzymes for dissociation of lung tissue [13], we have used type I collagenase for biopsy dissociation. The procedure to isolate human tumor bronchial cells from biopsies with type I collagenase is outlined in Figure 1F. We have assessed several concentrations and incubation times of type I collagenase (Figure 1G). Our results showed that the best efficiency was obtained with a concentration of 1,500 U of type I collagenase and a time of incubation of 2 hours. Once the cells are attached to the 12-well plate and start to divide to reach about 90% of confluence, cells are sub-cultured sequentially into 6-well plates and finally in flasks. Although these two methods presented in Figure 1B and 1H, yielded human lung epithelial tumor cells, the explants of human bronchial tumor biopsies appeared to give the greatest number of human lung epithelial tumor cells within the shortest time (Figure 1I).

*3.4 Morphological characteristics of purified human lung tumor cells.*

Structural characterization of human lung tumor cells showed the characteristic morphology of epithelial cells, such as an adherent monolayer, a cobblestone-like arrangement and a tightly packed pattern (Figure 1B). These primary human lung tumor epithelial cells obtained from biopsies have been maintained for 5 passages, and no obvious morphological change has been observed. Each cell appeared polygonal and flattened, with a large, round nucleus, typical features of normal epithelial cells (Figure 1B). To further characterize these human lung tumor epithelial cells, the expression of cytokeratin 18 (CK18) (an epithelial cell marker) [14, 15] (Figure 2A) and surfactant protein-C (SP-C) (a specific lung cell marker) [16] (Figure 2B) were analyzed at the 2nd passage for the phenotype of Cancer Lung Cells (CLC) from 4 different biopsies (CLC6, CLC1, CLC8, CLC7). The expression of the epithelial cell marker CK18 was examined by immunofluorescence, indicating the epithelial character of these cells (Figure 2A). Moreover, immunofluorescence staining showed that SP-C was expressed by all cells, for each patient, indicating the lung origin of these cells (Figure 2B). Taken together, these immunofluorescence results show that cells are positive both for epithelial and lung markers (Figure 2 A and B). Since one of the Cancer Lung cell line (CLC5) was expending very fast, we decided to further exploit this cell line. First, we validated by immunofluorescence these markers (CK18 and SP-C). CLC5 cells showed uniform positive immunofluorescence signals for CK18 (Figure 2C) and SP-C (Figure 2D). In contrast, immunofluorescence with a specific antibody against fibroblasts cell type did not show any indication of contamination of cultures by fibroblasts (α-SMA) (Figure 2E), and CLC5 are also negative for E-cadherin (Figure 2F). In NSCLC, several studies have reported a reduction of E-cadherin during malignant transformation [17]. Taken together, these results demonstrate that we have isolated human lung tumor cells from patient biopsies using the explant cell culture method.

Figure 2

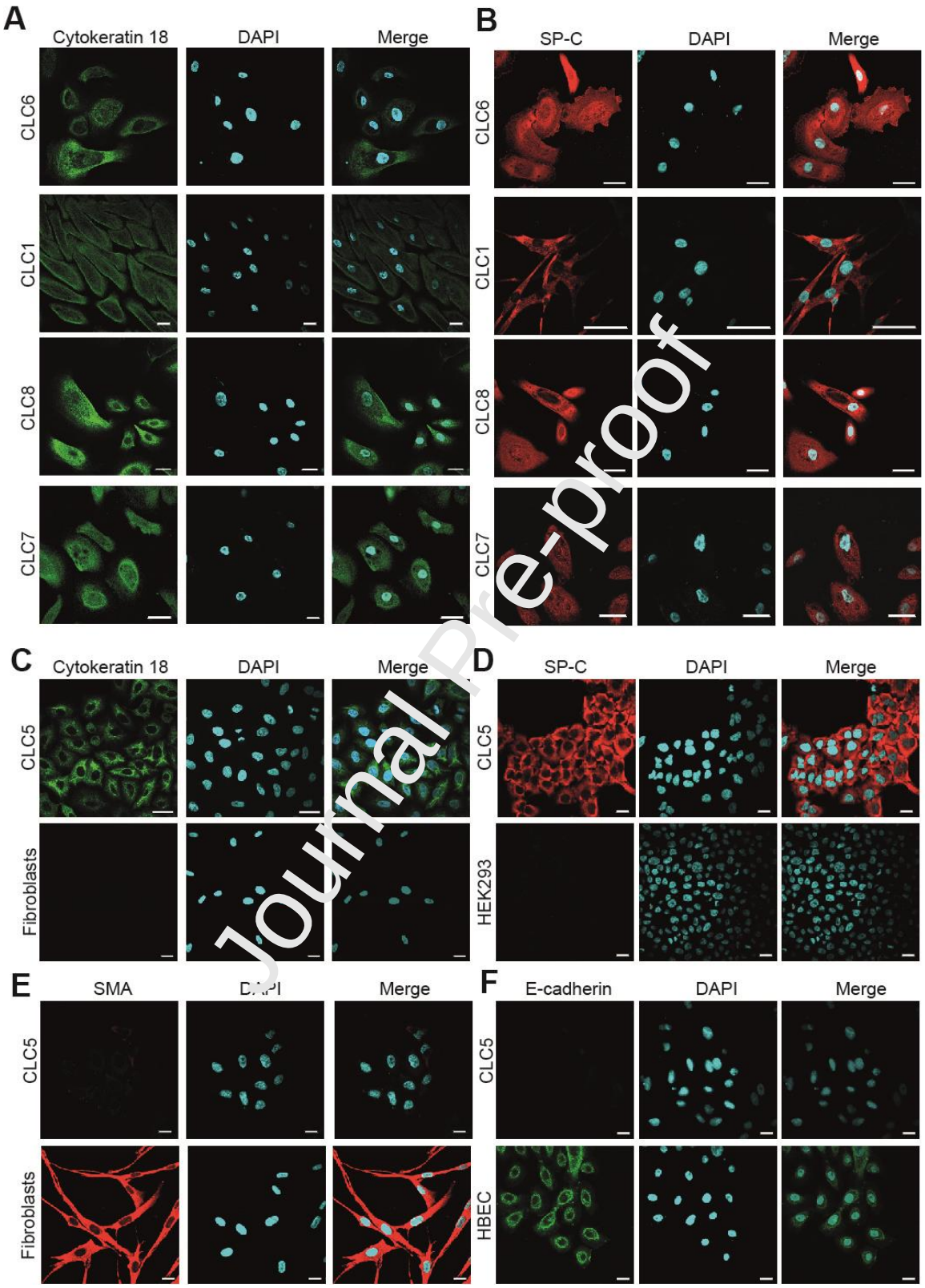




**Figure 2: Immunostaining of sub-cultured lung epithelial cells. A-D**, Primary cells from patients were seeded on a coverslip and fixed with 4% paraformaldehyde. Cells were stained with cytokeratin 18 (**A** and **C**) or surfactant protein C (SP-C) (**B** and **D**) and counterstained with DAPI for nuclei. **C-F**, CLC5

cells stained positive for cytokeratin 18 (**C**) and SP-C (**D**). Cultured lung cells did not stain for α-SMA (**E**), indicating no contamination of the primary cultured lung epithelial cells with mesenchymal cells and stained negative for E-cadherin/Alexa Fluor 546 (**F**). Positive control for α-SMA-cy3 is shown on fibroblasts (E). Positive control for E-cadherin is shown on HBEC epithelial cells (**F**). Scale Bar=100 µm. Images were acquired with the confocal microscope Nikon Eclipse 220-C1.

*3.5 PLDT establishment from patient-derived cell lines*

Previously, we have described the growth of cancer human bronchial epithelial cells in 3D basement membrane culture with Matrigel [10, 11]. By comparison between 3D architecture in normal and malignant cell lines, we were able to distinguish normal and malignant human bronchial cells [10, 11]. Our next objective was to compare the drug response in our two different culture systems (2D *vs* 3D) using the same 2D and 3D methods developed and characterized by our group [10]. Thus, we first established and monitored the 3D cell culture growth of CLC5 tumoroids and evaluated the size of tumoroids over time (Figure 3A). From day 1 to day 6, tumoroids were in an exponential growth phase and then reached a plateau at day 7 (Figure 3B). We then measured the size (diameter) and the number of tumoroids (Figure 3C-E) using Leica LasX software (see Materials and methods). We set up 10 classes of tumoroids of diameters ranging from 45 µm to 245 µm (Figure 3D).

**Figure 3**

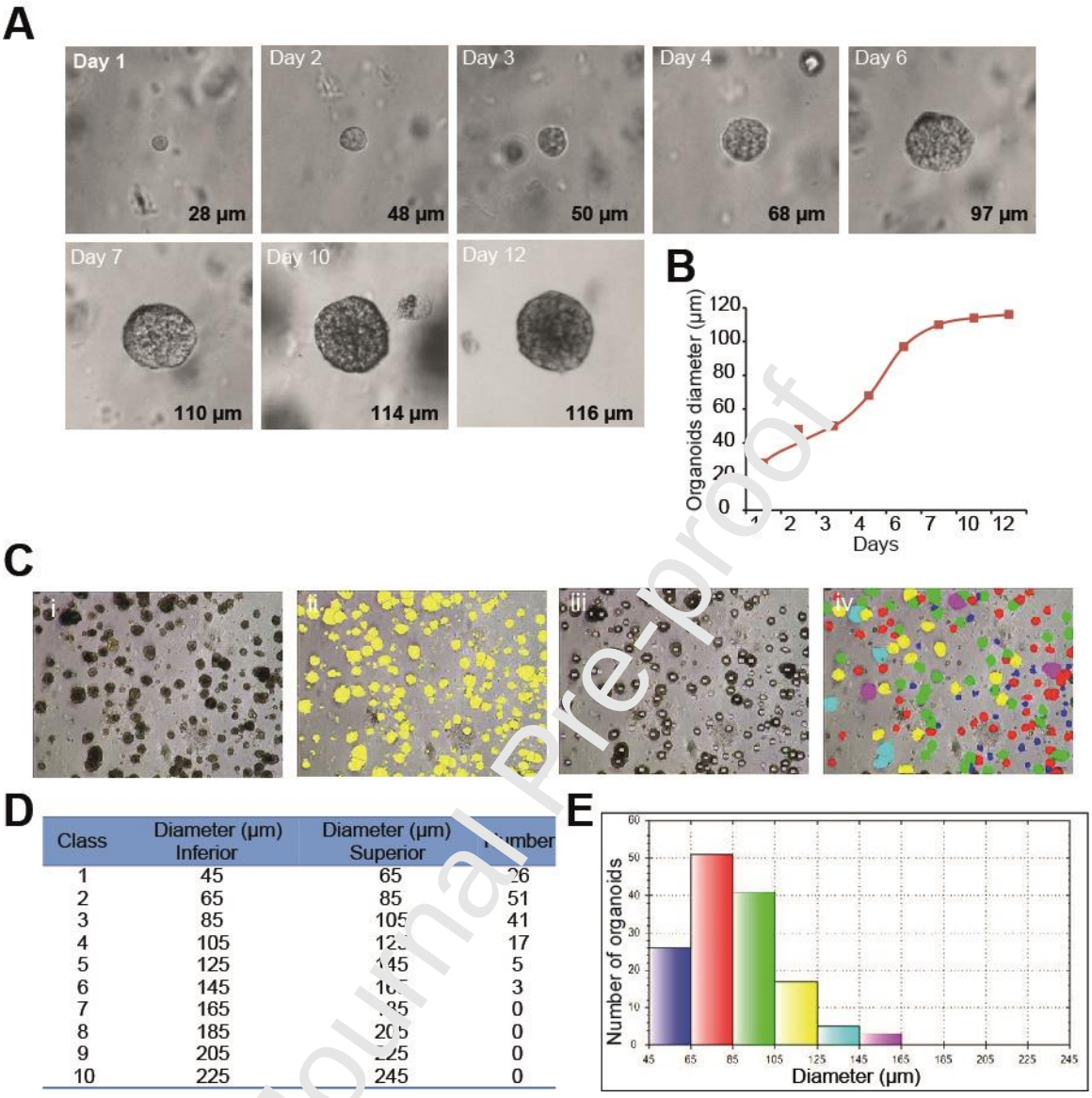


| Class | Diameter (µm) Inferior | Diameter (µm) Superior | Number |
|---|---|---|---|
| 1 | 45 | 65 | 26 |
| 2 | 65 | 85 | 51 |
| 3 | 85 | 105 | 41 |
| 4 | 105 | 125 | 17 |
| 5 | 125 | 145 | 5 |
| 6 | 145 | 165 | 3 |
| 7 | 165 | 185 | 0 |
| 8 | 185 | 205 | 0 |
| 9 | 205 | 225 | 0 |
| 10 | 225 | 245 | 0 |

**Figure 3: Tumoroids analysis setup. A**, Representative field of a tumoroid grown in 3D culture acquired by phase-contrast microscopy (Leica) at objective 5×. **B,** Analysis of the diameter of tumoroids followed every day until day 12. **C-E**, A binary treatment was applied to select the tumoroids to be analyzed (i-iv). The accounting software of the total tumoroids by classes (D) previously predefined (E) to measure the tumoroids according to their diameter.

*3.6 Drug sensitivity of 2D cultures as compared to 3D tumoroids (PLDTs).*

Next, we examine the drug sensitivity of 2D cultures from human lung tumor cells relative to their respective 3D PLDTs cultures. Figure 4A describes the strategy used to investigate differences between monolayer and PLDTs cultured tumor lines, obtained from lung cancer patient biopsies. To determine differences in drug sensitivity between cells cultured in 2D and cultured in a 3D matrix (PLDTs), we assessed the impact of chemotherapeutic drug treatments on cell viability. CLC5 cells were cultured in 2D monolayer and treated for 3 or 5 days with a dose ranging from 0 to 100 µM with Pemetrexed, Paclitaxel, Docetaxel, or Gemcitabine. Cell viability was then assessed upon exposure to different concentrations of the chemotherapeutic drugs for 3 and 5 days. As shown in Figure 4, the cell viability of CLC5 cells was reduced for each drug tested (Figure 4B-F) in a dose-dependent manner, with a remarkably strong effect for Gemcitabine (Figure 4F). Since Gemcitabine is the drug which has the best efficacy on the 2D cell viability (Figure 4F), we performed a soft agar colony formation assay to compare the effects of this agent on the ability of treated cells to divide and form colonies (Figure 4G). Cells treated with Gemcitabine had significantly less transformation than control cells ($P<0.0001$, Fig. 4H). These results demonstrated that Gemcitabine treatment effectively inhibited cell transformation at a dose similar to the one observed in the 2D cell viability assay.

Figure 4

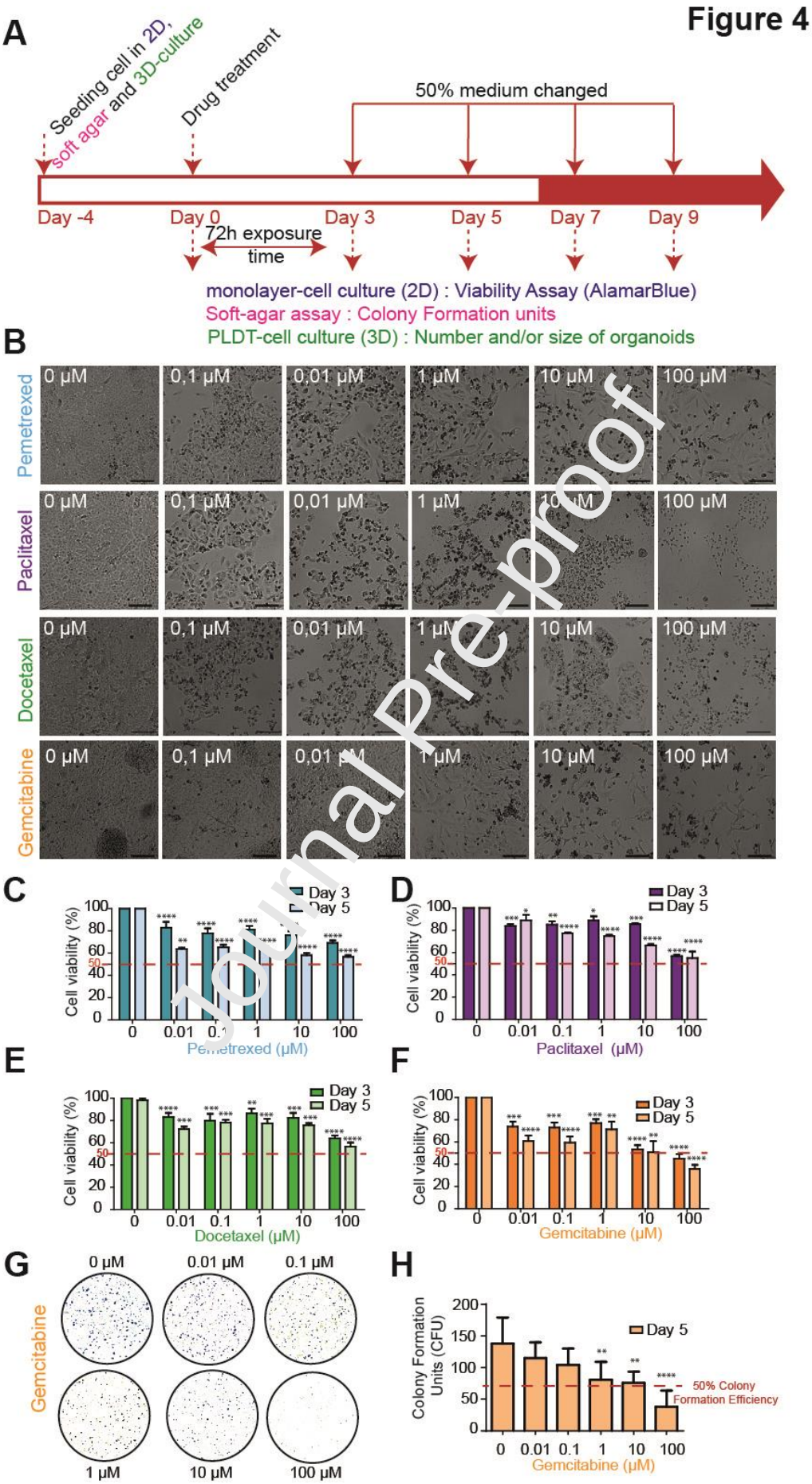

**Figure 4: Comparison of the effects of four chemotherapeutic agents on cell viability. A**, Timeline of the strategy used to measure the effects of the chemotherapeutic drugs in 2D and in 3D. **B-F**, Cells are seeded on 96-well plates to measure cell viability on 2D monolayer. Cells are treated with increasing doses ranging from 0 µM to 100 µM of Docetaxel, Paclitaxel, Gemcitabine, or Pemetrexed, respectively. Representative bright-field phenotype of the cells after drug exposure is shown in B. Scale bar=100 µm. **C-F**, Histograms measuring the 2D cell viability (mean ± s.e.m) following drug treatment from three independent biological replicates. The statistical analysis was performed between no treatment (0) and treated cells. * indicates $p<0.05$, ** indicates $p<0.001$ and ***indicates $p<0.001$ (Student's t-test). **G**, Soft agar colony formation in the presence of different doses of Gemcitabine. **H**, The graph shows the number of colonies (mean ± SEM.) after 3 weeks of three biological replicates. The p values (determined by Student's t test) are relative to control cells (0 µM). **$p\leq0.01$, ***$p\leq0.001$ and ****$p\leq0.0001$.

Our objective was to compare the drug sensitivity of 2D cultures from human lung tumor cells relative to their respective 3D PLDTs cultures. Our data showed that the anti-cancer Gemcitabine drug had the best efficacy on the 2D cell viability (reduction viability by 50% (Figure 4F)) and a very strongest effect on colony growth assay on soft agar (inhibition cellular transformation by 50% (Figure 4H)) on the CLC5 cells, thus, we have investigated the effect of this anti-cancer drug in our 3D model (PLDTs) to compare 2D vs 3D drug responses. Thereby, the impact of Gemcitabine in 3D tumoroid culture was evaluated and compared to the 2D culture (Figure 5). PLDTs from CLC5 were cultured with a dose ranging from 0 to 100 µM of Gemcitabine and the number and diameter of PLDTs were measured at 3, 5, and 7 days following treatment (Figure 5A-B). The number of PLDTs was significantly reduced in a dose-dependent manner (Figure 5B). In contrast, the diameter of PLDTs was not changed whatever the concentration of gemcitabine (data not shown). The cell viability rate of the CLC5 cell line in the presence of Gemcitabine was measured on day 3 and day 5 in 3D (Figure 5C) and 2D (Figure 5D) and the ratio of cell viability rates at day 5 was calculated (Figure 5 E). The $EC_{50}$ for the CLC5 cells following 3 days of treatment was $6.8\times10^{-7}$ M for 2D cultures and $1\times10^{-5}$ M for 3D cultures. We then tested the Gemcitabine effect on cell death in 2D as compared to 3D culture with drug (Gem) treatment. As shown in Supplemental Figure 1, cells were most susceptible to cell death when compared with control cells. The dose-dependent response of gemcitabine treatments was more effective in 2D than in 3D (Figure S1). We observed clearly different levels of sensitivity to Gemcitabine, translating into lower rates of survival when challenged with different drug amounts in 2D-culture (Figure 5E). Overall, cells grown in 3D tumoroids showed higher viability after treatment with increasing doses of gemcitabine compared with cells in 2D monolayer culture. The most straightforward explanation for drug resistance after Gemcitabine treatment in the tumoroids is that the cells inside the tumoroid are protected from drug accumulation. Taken together, our findings show that PLDT culture (3D) rather than monolayer culture (2D) better recapitulate the *in vivo* response.

**Figure 5**

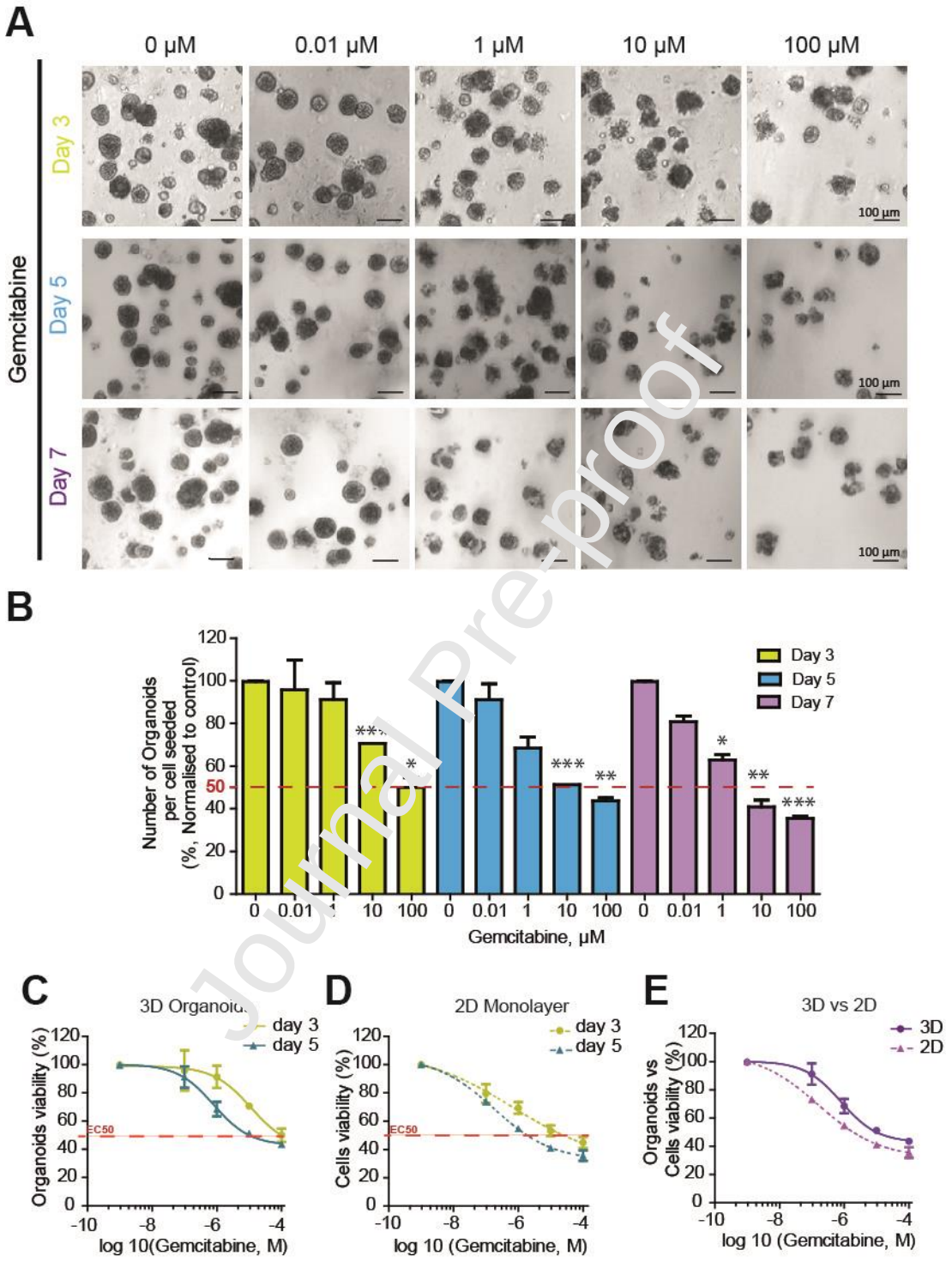


**Figure 5: Gemcitabine effect on PLDTs viability after 72 h, 120 h and 168 h of treatment**. **A,** Tumor epithelial cells were seeded in 3D culture in a 96-well plate. Cells were treated with different doses of Gemcitabine (0; 0.01; 1; 10 and 100 µM), and its effect was measured after 3, 5, and 7 days of treatment. Brightfield pictures were collected using a 10× objective. The scale bar corresponds to 100 µm. **B,** Analysis of gemcitabine response on 3D tumor organoids treated for 72 h with different doses of Gemcitabine or without treatment. Dose-response experiments are presented as a bar

graph using GraphPad Prism software. Each point is the mean ± SD of 3 biological replicates. The statistical analysis was performed between no treatment and treated cells. * indicates $p<0.05$, ** indicates $p<0.001$ and ***indicates $p<0.001$. **C-D**, Gemcitabine dose-response curve in 3D tumor organoids and 2D monolayers following 3 days and 5 days of treatment. Dose-response experiments are presented using GraphPad Prism software. Each point is the mean ± SD of at least 3 biological replicates. **E**, Comparison of gemcitabine dose-response curve between 3D tumoroids and 2D cell monolayers following 5 days of treatment. Dose-response experiments are presented using GraphPad Prism software. Each point is the mean ± SD of at least 3 biological replicates.

*3.7 Identification of differential response of PLDTs to Gemcitabine and/or radiation.*

Chemotherapy and radiation are standard treatments for patients with locally advanced lung cancer. Thus, we sought to analyze the differential response of 2D monolayers as compared to PLDTs treated with chemotherapy and radiation. 2D cell monolayer and tumoroids were grown in feeding media for 96 hours prior to treatment. Baseline brightfield images were acquired prior to treatment with Gemcitabine (0, 1, and 10 µM) and radiation (0, 2, or 5 Gy). Cells were exposed to Gemcitabine for 72 h hours and radiation once. Brightfield imaging was performed again after 3 and 5 days (Figure 6A, D, G, J). Change in diameter of individual tumoroids was measured and compared across samples and treatment conditions as a marker of PLDTs growth response (Figure 6B, E, H, K). A significant variation in the cell viability response to Gemcitabine and radiation was observed across samples for both radiation and the gemcitabine dose tested (Figure 6C, F, I, L). LC5 were responsive to both Gemcitabine and radiation with increasing concentrations of Gemcitabine and increased radiation dose as evidenced by a significant reduction in means tumoroids size (PLDT Mean Growth, Figure 6 B, E, H, K), and in cell viability both in 2D and in 3D (Figure 6 C, F, J, L). These results indicate a high effect on cellular viability after treatment with Gemcitabine combined with 2-Gy and 5-Gy radiation. The highest effect was after 5-Gy radiation and subsequent Gemcitabine treatments.

**Figure 6**

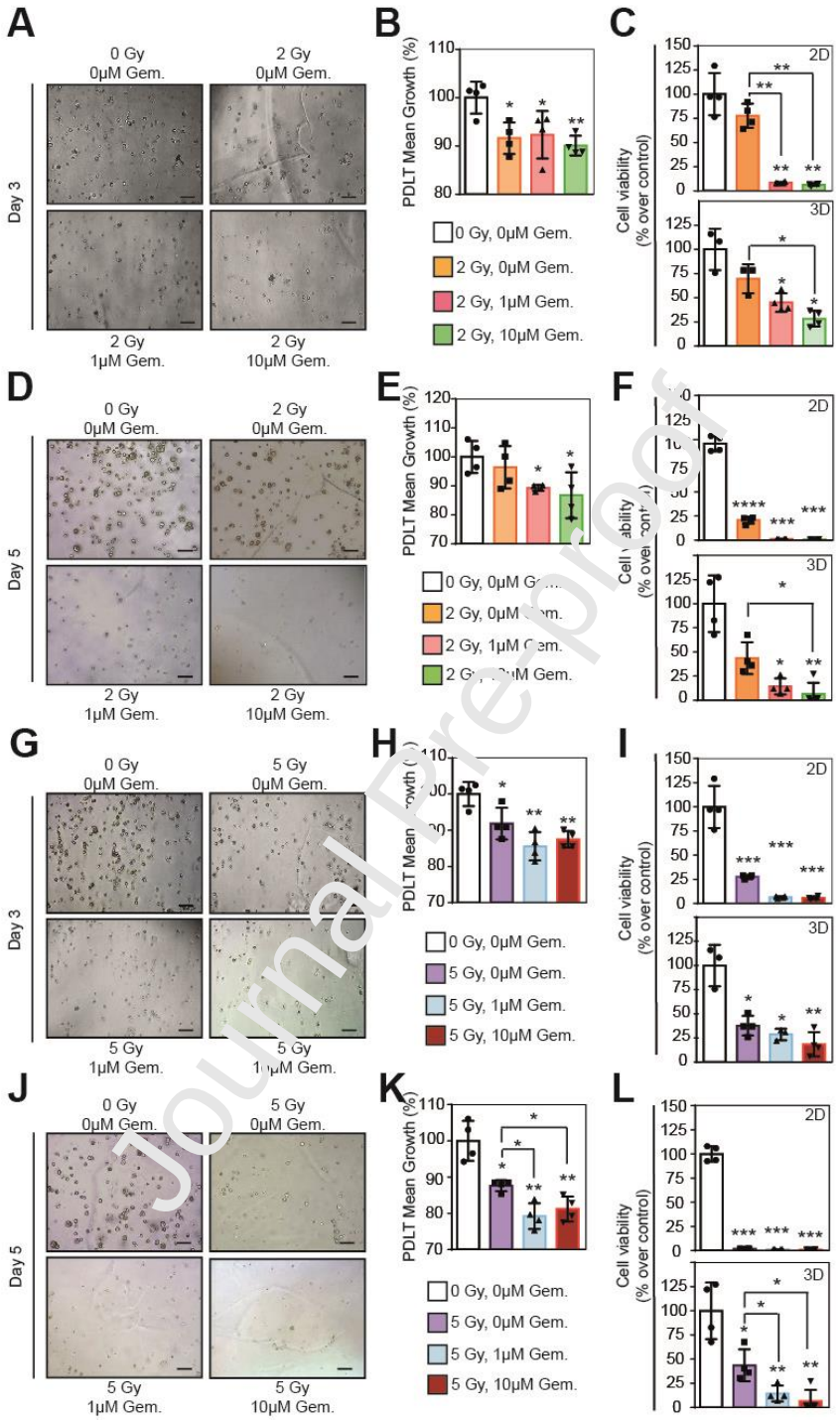


**Figure 6: Responses to combined treatment of Gemcitabine and radiation using PLDTs. A,D,G,J**, PLDTs were treated with increasing doses of Gemcitabine and/or radiation (0, 2, or 5 Gy) and then PLDTs were observed over 3 and 5 days. Brightfield images are for PLDTs treated with control (vehicle), 1 or 10 µM Gemcitabine and 2 or 5-Gy radiation baseline and 3 or 5 days post-treatment. Scale bar=100 µm. **B, E, H, K,** Mean tumoroids growth (%) was measured for the different treatment conditions. Growth is defined as a change in tumoroid diameter. **C, F, I, L,** Analysis of radiation and or

Gemcitabine responses on cell viability in 2D as compared to 3D tumoroids treated for 3 and 5 days. Cell viability is presented as a bar graph using GraphPad Prism software. Each point is the mean ± SEM of at least 4 biological replicates. *p<0.05, **p<0.01, **p<0.001, ***p<0.0001 and ****p<0.0001 (Student's t-test).

## 4 Discussion

Human cell-based models are required for determining relevant pathways involved in human lung cancer mechanisms and for developing cell-based *in vitro* screening of new drugs, leading to early evaluation and better success rates. Personalized lung cancer medicine is devoted to tailoring the most appropriate drug to be prescribed to individual patients. To achieve this goal, genomic-based drug response prediction has enabled better decision making in oncology. However, evaluating the functionality of these predictions is difficult because of the lack of representative patient lung tumor models that can recapitulate all the key features of original tumors.

Here, we showed that PLDTs have great potential for predicting clinical responses to drugs and for selecting treatments. This type of culture has been previously shown to maintain the features of cancers from which they derived, including genetic and metabolic alterations, and also drug responses [12]. In this study, we presented detailed methods for culturing and expand primary human lung tumor epithelial cells from biopsy. We obtained lung cancer explants, freshly collected by biopsy and confirmed by immunofluorescence for the presence of specific human lung tumor epithelial cells, and tried to establish lung cancer cell lines from twelve patients' tumors (CLC1 to CLC12). The efficiency of PLDT lines establishment from biopsies was 75% (9 lines from 12 ''attempts'' from cancer biopsies) and could presumably be improved by further optimization of growth conditions. We demonstrated how explants of bronchial tumor tissue, cultured in media that promote epithelial cell growth, can provide a continuous source of human lung tumor epithelial cells.

These human lung tumor cells can be utilized in drug testing systems that more closely resemble cells living in their actual physiologic environment. Cell-cell and cell-ECM interactions observed during *in vivo* tumor progression cannot be studied in 2D models, whereas the 3D models are capable of mimicking these conditions. Consequently, various lung cancer cell lines have been tested in the literature for their ability to grow as tumoroids in 3D culture [10, 18]. Thus, in this study, we have investigated and showed that 3D cultures of human lung epithelial tumor cell lines are generally more resistant to chemo- and radio-therapy than their 2D counterparts. Anticancer effects of various chemotherapeutic agents were studied and conventional 2D and 3D cell cultures were compared. Chemo-resistance in tumors is mediated by various mechanisms. The classical mechanisms are based on ATP-binding cassette (ABC) transporter proteins, such as ABCC5 (MRP5)[19], which have been reported to contribute to chemo-resistance [20]. High-affinity uptake of gemcitabine is basically mediated by the pyrimidine-preferring nucleoside transporter hCNT1 and also hENT1 which plays a role in drug uptake [21]. Thus we cannot exclude the possibility that

nucleoside transporters would significantly contribute to gemcitabine cytotoxicity, especially in lung tumor types in which this drug is currently used. This remains to be elucidated.

However, validated 3D *in vitro* lung cell models have not been developed for rapid and standardized screening of chemo- and radio-resistance. A combined measure using the change of tumoroid size and number appears to be a robust measure of response for studying chemo-resistance mechanisms.

One of the goals of this work was also to gain further experience using PLDTs to predict the effectiveness of chemotherapy and radiation for patients with lung cancer. In the present study, gemcitabine and irradiation treatment were more effective in monolayers as compared to PLDT. Combination treatment led to both a significant decrease in cell viability and PLDT growth.

We found that 3D tumoroids are substantially more resistant to radiation than monolayer cultures, with a dose modification factor of 3 for 2-Gy radiation and 25 for 5-Gy radiation. This is probably due to factors characteristic of tumoroids, such as the presence of hypoxic cells and of a high proportion of non-proliferating cells. As hypoxia is thought to be a major factor responsible for the radioresistance of tumor cells [22], it is possible that hypoxic regions in tumoroids might influence the effects of radiation. However, in some studies, the correlation between radioresistance and hypoxia was not evident [23, 24], suggesting that other factors such as cell-cell contact and the importance of the fraction of non-proliferating cells might play a more important role in radiation outcome. This remains elusive.

In addition to its cytotoxic effect, Gemcitabine is a potent radiosensitizer [25, 26]. Gemcitabine is activated by nucleoside kinases into two compounds, gemcitabine diphosphate (dFdCDP) and gemcitabine triphosphate (dFdCTP) [27]. Gemcitabine diphosphate (dFdCDP) has been shown to inhibit ribonucleotide reductase, which is responsible for catalyzing the reactions that generate the deoxynucleotides required for DNA synthesis and repair; whereas gemcitabine triphosphate competes with dCTP for incorporation into DNA during replication, which results in a termination of chain elongation [27]. The mechanism of radio-sensitization or radio-enhancement by gemcitabine has been associated with the depletion of the dATP pools, the accumulation of cells in S phase of the cell cycle, the p53 status, the induction of apoptosis, the increase of DNA double-strand breaks, and the modification of DNA repair pathways [28]. Herein, we showed that gemcitabine can enhance the effects of irradiation in both 2D and 3D tumoroids, while the effect was more pronounced in 2D. Although, a critical limitation remains from this model is the lack of a cancer microenvironment including stromal cells and immune cells, because tumoroids are derived only from human lung epithelial cancer cells. Thus, to investigate the interaction between cancer cells and

the microenvironment, a co-culture system with immune/stromal cells should be developed in the next future.

In conclusion, we established a PDLTs model that will be a useful platform for drug screening and new clinical trials. Additionally, considering the short length of time from the model establishment to drug testing, our model can be used for predicting patient-specific drug responses as well as broader preclinical studies. Therefore, the ability to predict outcomes in preclinical animal experiments and clinical trials can be better understood using 3D cultures, which is a potentially useful predictive tool in the clinical setting for drug screening in the future. Using PLDTs cultures from surgical patients can be expanded to various fields of drug sensitivity testing, radiosensitivity testing, and novel drug delivery approaches for personal therapeutic strategies of lung cancer patients.

**Acknowledgements**

We gratefully acknowledge the members from the ARTiSt group for their critical remarks. This work was supported by grants from the “Région Nouvelle-Aquitaine”. FD was supported by grants from the “Fondation ARC pour la Recherche sur le Cancer”. DF has been supported by the “Agence Nationale de la Recherche (ANR)”. TG was supported by the “SIRIC Brio”. We would like to acknowledge Marie-Alix Derieppe for help in setting up the radiation experiment.

## 5 References

[1] J. Yokota, T. Kohno, Molecular footprints of human lung cancer progression, Cancer science, 95 (2004) 197-204.
[2] W.D. Travis, E. Brambilla, P. Van Schil, G.V. Scagliotti, R.M. Huber, J.P. Sculier, J. Vansteenkiste, A.G. Nicholson, Paradigm shifts in lung cancer as defined in the new IASLC/ATS/ERS lung adenocarcinoma classification, The European respiratory journal, 38 (2011) 239-243.
[3] W.D. Travis, Pathology of lung cancer, Clinics in chest medicine, 32 (2011) 669-692.
[4] Y. Sekido, K.M. Fong, J.D. Minna, Molecular genetics of lung cancer, Annual review of medicine, 54 (2003) 73-87.
[5] A. Dutt, K.K. Wong, Mouse models of lung cancer, Clinical cancer research : an official journal of the American Association for Cancer Research, 12 (2006) 4396s-4402s.
[6] L. Hutchinson, R. Kirk, High drug attrition rates--where are we going wrong?, Nature reviews. Clinical oncology, 8 (2011) 189-190.
[7] W.N. Hait, Anticancer drug development: the grand challenges, Nature reviews. Drug discovery, 9 (2010) 253-254.
[8] H.B. van der Worp, D.W. Howells, E.S. Sena, M.J. Porritt, S. Rewell, V. O'Collins, M.R. Macleod, Can animal models of disease reliably inform human studies?, PLoS medicine, 7 (2010) e1000245.
[9] A.C. Rios, H. Clevers, Imaging organoids: a bright future ahead, Nature methods, 2018, pp. 24-26.
[10] D. Fessart, H. Begueret, F. Delom, Three-dimensional culture model to distinguish normal from malignant human bronchial epithelial cells, The European respiratory journal, 42 (2013) 1345-1356.
[11] D. Fessart, C. Domblides, T. Avril, L.A. Eriksson, H. Begueret, R. Pineau, C. Malrieux, N. Dugot-Senant, C. Lucchesi, E. Chevet, F. Delom, Secretion of protein disulphide isomerase AGR2 confers tumorigenic properties, eLife, 5 (2016).
[12] M. Kim, H. Mun, C.O. Sung, E.J. Cho, H.J. Jeon, S.M. Chun, D.J. Jung, T.H. Shin, G.S. Jeong, D.K. Kim, E.K. Choi, S.Y. Jeong, A.M. Taylor, S. Jain, M. Meyerson, S.J. Jang, Patient-derived lung cancer organoids as in vitro cancer models for therapeutic screening, Nature communications, 10 (2019) 3991.
[13] J.G. Quatromoni, S. Singhal, P. Bhojnagarwala, W.W. Hancock, S.M. Albelda, E. Eruslanov, An optimized disaggregation method for human lung tumors that preserves the phenotype and function of the immune cells, Journal of leukocyte biology, 97 (2015) 201-209.
[14] T. Makino, M. Yamasaki, A. Takeno, M. Shirakawa, H. Miyata, S. Takiguchi, K. Nakajima, Y. Fujiwara, T. Nishida, N. Matsuura, M. Mori, Y. Doki, Cytokeratins 18 and 8 are poor prognostic markers in patients with squamous cell carcinoma of the oesophagus, British journal of cancer, 101 (2009) 1298-1306.
[15] V. Barak, H. Goike, K.W. Panaretakis, R. Einarsson, Clinical utility of cytokeratins as tumor markers, Clinical biochemistry, 37 (2004) 529-540.
[16] C.F. Kim, E.L. Jackson, A.E. Woolfenden, S. Lawrence, I. Babar, S. Vogel, D. Crowley, R.T. Bronson, T. Jacks, Identification of bronchioalveolar stem cells in normal lung and lung cancer, Cell, 121 (2005) 823-835.
[17] N.H. Myong, Reduced expression of E-cadherin in human non-small cell lung carcinoma, Cancer research and treatment : official journal of Korean Cancer Association, 36 (2004) 56-61.
[18] N. Sachs, A. Papaspyropoulos, D.D. Zomer-van Ommen, I. Heo, L. Bottinger, D. Klay, F. Weeber, G. Huelsz-Prince, N. Iakobachvili, G.D. Amatngalim, J. de Ligt, A. van Hoeck, N. Proost, M.C. Viveen, A. Lyubimova, L. Teeven, S. Derakhshan, J. Korving, H. Begthel, J.F. Dekkers, K. Kumawat, E. Ramos, M.F. van Oosterhout, G.J. Offerhaus, D.J. Wiener, E.P. Olimpio, K.K. Dijkstra, E.F. Smit, M. van der Linden, S. Jaksani, M. van de Ven, J. Jonkers, A.C. Rios, E.E. Voest, C.H. van Moorsel, C.K. van der Ent, E. Cuppen, A. van Oudenaarden, F.E. Coenjaerts, L. Meyaard, L.J. Bont, P.J. Peters, S.J. Tans, J.S. van Zon, S.F. Boj, R.G. Vries, J.M. Beekman, H. Clevers, Long-term expanding human airway organoids for disease modeling, The EMBO journal, 38 (2019).

[19] W. Hagmann, R. Jesnowski, J.M. Lohr, Interdependence of gemcitabine treatment, transporter expression, and resistance in human pancreatic carcinoma cells, Neoplasia, 12 (2010) 740-747.
[20] A. Domenichini, A. Adamska, M. Falasca, ABC transporters as cancer drivers: Potential functions in cancer development, Biochimica et biophysica acta. General subjects, 1863 (2019) 52-60.
[21] J. Garcia-Manteiga, M. Molina-Arcas, F.J. Casado, A. Mazo, M. Pastor-Anglada, Nucleoside transporter profiles in human pancreatic cancer cells: role of hCNT1 in 2',2'-difluorodeoxycytidine-induced cytotoxicity, Clinical cancer research : an official journal of the American Association for Cancer Research, 9 (2003) 5000-5008.
[22] R.M. Sutherland, Tumor hypoxia and gene expression--implications for malignant progression and therapy, Acta oncologica, 37 (1998) 567-574.
[23] A. Gorlach, H. Acker, pO2- and pH-gradients in multicellular spheroids and their relationship to cellular metabolism and radiation sensitivity of malignant human tumor cells, Biochimica et biophysica acta, 1227 (1994) 105-112.
[24] F.M. Buffa, C. West, K. Byrne, J.V. Moore, A.E. Nahum, Radiation response and cure rate of human colon adenocarcinoma spheroids of different size: the significance of hypoxia on tumor control modelling, International journal of radiation oncology, biology, physics, 49 (2001) 1109-1118.
[25] D.S. Shewach, T.S. Lawrence, Gemcitabine and radiosensitization in human tumor cells, Investigational new drugs, 14 (1996) 257-263.
[26] T.S. Lawrence, A. Eisbruch, D.S. Shewach, Gemcitabine-mediated radiosensitization, Seminars in oncology, 24 (1997) S7-24-S27-28.
[27] P.A. Risbood, C.T. Kane, Jr., M.T. Hossain, S. Vadapalli, S.K. Chadda, Synthesis of gemcitabine triphosphate (dFdCTP) as a tris(triethylammonium) salt, Bioorganic & medicinal chemistry letters, 18 (2008) 2957-2958.
[28] B. Pauwels, A.E. Korst, F. Lardon, J.B. Vermorken, Combined modality therapy of gemcitabine and radiation, The oncologist, 10 (2005) 34-51.

Table 1 : Patients' characteristics

| Patients | Gender | Age | Histology | *EGFR* Exons 18-21 | *KRAS* Exon 2 | *ERBB2* Exon 20 | *ALK* | *ROS1* | *BRAF* Exon 15 |
|---|---|---|---|---|---|---|---|---|---|
| **CLC1** | M | 74 | Adenocarcinoma | - | p.G12C | - | - | - | - |
| **CLC2** | F | 61 | Adenocarcinoma | - | - | - | - | - | - |
| **CLC3** | F | 64 | Adenocarcinoma | Exon 21 p.L858R | - | - | - | - | - |
| **CLC4** | M | 59 | Squamous cell carcinoma | - | - | - | - | - | - |
| **CLC5** | M | 79 | Adenocarcinoma | - | - | - | - | - | - |
| **CLC6** | F | 58 | Adenocarcinoma | - | p.G12C | - | - | - | - |
| **CLC7** | F | 62 | Adenocarcinoma | Exon 20 Exon 21 | - | - | - | - | - |
| **CLC8** | F | 83 | Adenocarcinoma | - | p.G12V | - | - | - | - |
| **CLC9** | M | 45 | Adenocarcinoma | - | p.G12V | - | - | - | - |
| **CLC10** | F | 69 | Adenocarcinoma | - | p.G12V | - | - | - | - |
| **CLC11** | M | 63 | Adenocarcinoma | - | - | - | - | - | - |
| **CLC12** | M | 66 | Adenocarcinoma | - | - | - | - | - | - |

## Supplemental Figure 1

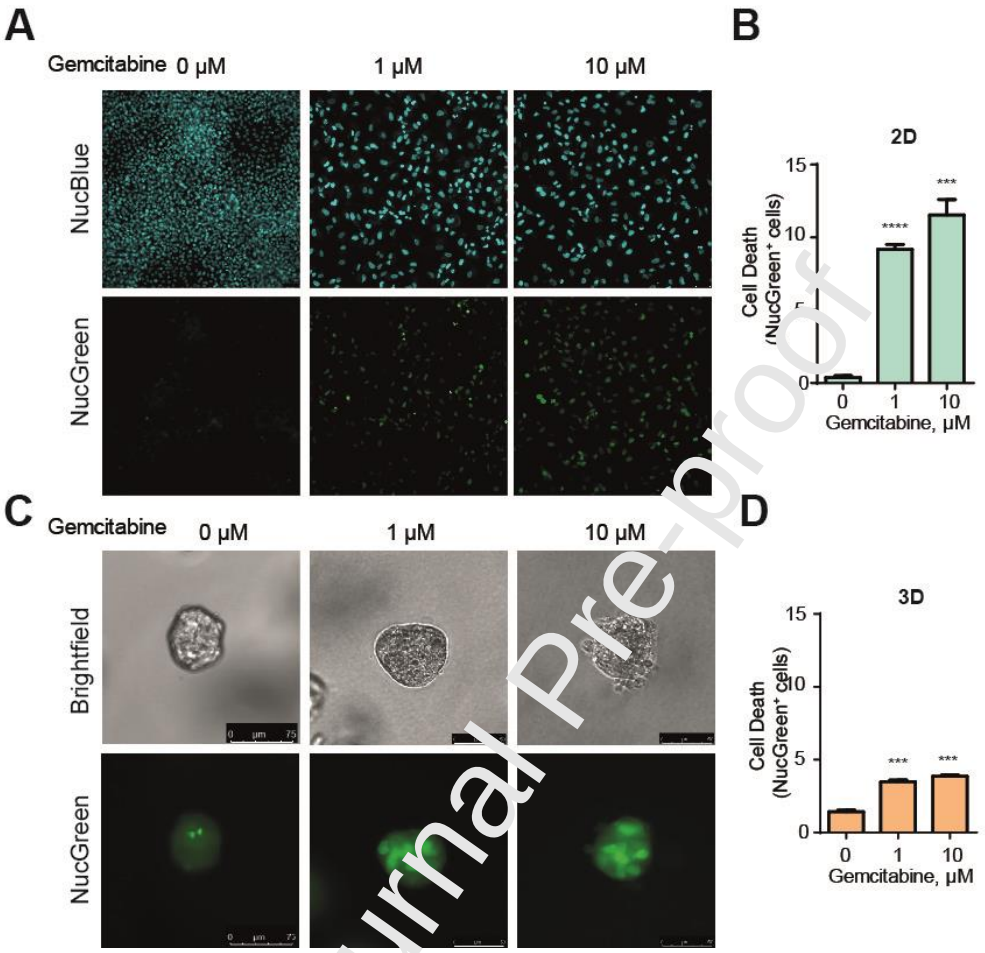


**Supplemental Figure 1: Cell death using NucGreen staining of Gemcitabine-treated cells grown as monolayers as compared to tumoroids. A-B**, Representative images of 2D monolayer seeded for 4 days and treated with Gemcitabine at different doses in the presence of NucGreen (a marker of dead cells) and Nucblue (nuclei marker) as described in Materials and methods. The images were then acquired at 4× magnification and fluorescence signals were then quantified to obtain the graph (B). Scale bars indicate 1000 µm. **C-D**, Representative images of 3D tumoroids grown for 4 days in Matrigel and treated with Gemcitabine at different doses in the presence of NucGreen (a marker of dead cells) as described in materials and methods. The images were then acquired at 4× magnification and fluorescence signals were then quantified to obtain graph (D). Scale bars indicate the length in µm. Each point is the mean ± SEM of at least 3 biological replicates. ***p<0.0001 and ****p<0.0001 (Student's t-test) relative to control condition (dose 0).

**Declaration of interest**

None

**Authors' contributions**

DF, IB, TG, FS and FD carried out the experiments and related analyses. GS and AMK provided the reagents and critically revised the manuscript. HB provided and analyzed the biopsies. JR critically revised the manuscript. FD, DF designed the study and wrote the manuscript. All authors read and approved the final manuscript.

**Declaration of interests**

☒ The authors declare that they have no known competing financial interests or personal relationships that could have appeared to influence the work reported in this paper.

☐The authors declare the following financial interests/personal relationships which may be considered as potential competing interests:

**CRediT author statement**

**DF, IB, TG, FS and FD** carried out the experiments and related analyses. **GS and AMK** provided the reagents and critically revised the manuscript. **HB** provided and analyzed the biopsies. **JR** critically revised the manuscript. **FD, DF** designed the study and wrote the manuscript. All authors read and approved the final manuscript.

**HIGHLIGHTS**

- Establishment of tumoroids derived from lung cancer patients (PLDT) as a platform for drug screening
- PLDT are more resistant to chemotherapeutic drug that cells in 2D culture.
- Gemcitabine can enhance the effects of irradiation in both 2D and 3D tumoroids